Electronic Supplementary Material

Radiofluorinated GPC3-Binding Peptides for PET Imaging of Hepatocellular Carcinoma

Journal: Molecular Imaging and Biology

Youcai Li [1,3,§], Jun Zhang [2,4,§], Jiamei Gu [1], Kongzhen Hu [1], Shun Huang [1], Peter S. Conti [2], Hubing Wu [1,2,*], Kai Chen [2,*]

[1]*Nanfang PET Center, Nanfang Hospital, Southern Medical University, Guangzhou, Guangdong Province, China*

[2]*Molecular Imaging Center, Department of Radiology, Keck School of Medicine, University of Southern California, Los Angeles, CA 90033, USA*

[3]*PET/CT Center, The First Affiliated Hospital of Guangzhou Medical University, Guangzhou, Guangdong Province, China*

[4]*Department of Nuclear Medicine, Taizhou People's Hospital, Taizhou, Jiangsu Province, China*

*Corresponding authors:

Nanfang PET Center, Nanfang Hospital, Southern Medical University, 1838 Guangzhou Avenue North, Guangzhou, Guangdong Province, China, 510515. Tel: +86-20-62787317; Fax: +86-20-61642127; E-mail: wuhbym@163.com (H. Wu)

Molecular Imaging Center, Department of Radiology, Keck School of Medicine, University of Southern California, 2250 Alcazar Street, CSC103, Los Angeles, CA 90033. Tel: +1-323-442-3858; Fax: +1-323-442-3253; E-mail: chenkai@med.usc.edu (K. Chen)

§These authors contributed equally to this work.

General

All chemicals were obtained from commercial suppliers and used without further purification. The peptides (sequence: RLNVGGTYFLTTRQ and GGGRDNRLNVGGTYFLTTRQ) were synthesized by the ChinaPeptides Company (Shanghai, China). 2, 2', 2''-(2-(4-isothiocyanatobenzyl)-1,4,7-triazonane-1,4,7-triyl)triacetic acid (*p*-SCN-Bn-NOTA) was purchased from the AREVA Med Company (Plano, TX, USA). An anti-GPC3 antibody (Rabbit polyclonoal) was obtained from Abcam Company (Shanghai, China). [^{18}F]Fluoride was produced via the ^{18}O(p,n)^{18}F nuclear reaction with a General Electric (GE) PETtrace cyclotron (GE Healthcare, USA). Reverse-phase extraction C_{18} Sep-Pak cartridges were purchased from Waters (Milford, MA, USA). The cartridges were pre-conditioned with ethanol and water prior to use. HepG2 hepatocellular carcinoma (HCC) (GPC3-positive) cells and McA-RH7777 HCC (GPC3-negative) cells were obtained from the Institute of Biochemistry and Cell Biology, Shanghai Institutes for Biological Sciences, Chinese Academy of Sciences (Shanghai, China). All animal experiments were conducted in accordance with the guideline of the Nanfang Hospital Animal Ethics Committee at the Southern Medical University. Male or female BALB/c nude mice (about 4–6 weeks old) were obtained from the Laboratory Animal Center at Southern Medical University.

HPLC Methods

Semi-preparative reversed phase high-performance liquid chromatography (HPLC) for GP2076 or GP2633 was performed on a ThermoFisher UltiMate 3000 HPLC system using a Phenomenex Luna C18 reversed phase column (5 μm, 250 × 10 mm). The flow rate was 4 mL/min, with the mobile phase starting from 95% solvent A (0.1% trifluoroacetic acid (TFA) in water) and 5% solvent B (0.1% TFA in acetonitrile) to 40% solvent A and 60% solvent B during 25.5 min. The UV absorbance was monitored at 214 nm and 254 nm. The radiolabeled peptides were identified using an analytic HPLC system (Shimadzu, Japan) consisting of a Shimadzu LC-10AD pump, a variable wavelength SPD-M20A UV detector, and a Flow Count radio-HPLC Detector (Bioscan). The UV absorbance was monitored at 214 and 254 nm. The analytic HPLC was performed on a ZORBAX Eclipse XDB-C18 column (5 μm, 150 × 4.6

mm). The flow rate was 1 mL/min with the mobile phase starting from 95% solvent A (0.1% TFA in water) to 20% solvent A and 80% solvent B (0.1% TFA in acetonitrile) during 25 min.

Synthesis of GP2076

The peptide [RLNVGGTYFLTTRQ] (2.0 mg, 1.23 μmol) dissolved in 0.5 mL of sodium borate buffer (pH 8.5) was mixed with *p*-SCN-Bn-NOTA (0.7 mg, 1.25 μmol) in 20 μL of DMSO. The pH of mixture was adjusted to 8.5 using 0.1 M NaOH. After sonication at 40°C for 2 h, the mixture was dissolved in water and purified by semi-preparative HPLC. The peak containing the GP2076 peptide was collected and lyophilized to afford fluffy white powder (1.9 mg, yield: 74%). ESI-MS m/z $C_{92}H_{142}N_{26}O_{27}S$: $[M + 2H]^{2+}$ calcd, 1039.17, found, 1039.05; $[M + 3H]^{3+}$ calcd, 693.11, found, 693.07.

Synthesis of Al[^{19}F]F-GP2076

To a 1 mL V-vial containing 0.2 mL of deionized water were added 10 μl of 2 mM aluminum chloride in 0.1 M sodium acetate buffer (pH 4.0) and 7 μl of 3 mM sodium fluoride in 0.1 M sodium acetate buffer (pH 4.0). The mixture was heated at 100°C for 10 min. To the reaction mixture, 5 μl of 2.5 mM GP2076 in 0.1 M sodium acetate buffer (pH 4.0) was added, and the mixture was heated at 100°C for additional 10 min. The mixture was cooled and then purified by semi-preparative HPLC. The peak containing the Al[^{19}F]F-GP2076 peptide was collected. ESI-MS m/z $C_{92}H_{140}AlFN_{26}O_{27}S$: $[M + 2H]^{2+}$ calcd, 1061.15, found, 1061.07; $[M + 3H]^{3+}$ calcd, 707.77, found, 707.84.

Synthesis of GP2633

The peptide [GGGRDNRLNVGGTYFLTTRQ] (2.6 mg, 1.0 μmol) dissolved in 0.5 mL of sodium borate buffer (pH 8.5) was mixed with *p*-SCN-Bn-NOTA (0.6 mg, 1.07 μmol) in 20 μL of DMSO. The pH of mixture was adjusted to 8.5 using 0.1 M NaOH. After sonication at 40°C for 2 h, the mixture was dissolved in water and purified by semi-preparative HPLC. The peak containing the GP2633 peptide was collected and lyophilized to afford fluffy white powder (1.8 mg, yield: 68%). ESI-MS m/z $C_{112}H_{174}N_{36}O_{36}S$: $[M + 2H]^{2+}$ calcd, 1317.43, found,

1317.54; $[M + 3H]^{3+}$ calcd, 878.62, found, 878.51.

Synthesis of Al[^{19}F]F-GP2633

To a 1 mL V-vial containing 0.2 mL of deionized water were added 10 μl of 2 mM aluminum chloride in 0.1 M sodium acetate buffer (pH 4.0) and 7 μl of 3 mM sodium fluoride in 0.1 M sodium acetate buffer (pH 4.0). The mixture was heated at 100°C for 10 min. To the reaction mixture, 5 μl of 2.5 mM GP2633 in 0.1 M sodium acetate buffer (pH 4.0) was added, and the mixture was heated at 100°C for additional 10 min. The mixture was cooled and then purified by semi-preparative HPLC. The peak containing the Al[^{19}F]F-GP2633 peptide was collected. ESI-MS m/z $C_{112}H_{172}AlFN_{36}O_{36}S$: $[M + 3H]^{3+}$ calcd, 893.28, found, 893.40.

Measurement of Lipophilicity (Log P)

Approximately 185 kBq of Al[^{18}F]F-GP2076 or Al[^{18}F]F-GP2633 in 0.5 ml of phosphate-buffered saline (PBS) (pH 7.4) was mixed with 0.5 ml of 1-octanol. The mixture was vigorously shaken for 1 min, and then centrifuged at 12,000 rpm for 5 min to partition the organic and aqueous layers. Aliquots of 0.2 ml each layer were taken and the radioactivity was determined by gamma counting (GC-1200, USTC Chuangxin Co. Ltd. Zonkia Branch, China). The distribution coefficient P was calculated as the ratio of radioactivity in the organic phase to that in the aqueous phase. The experiment was carried out in quadruplicate.

Cell Culture and Animal Models

HepG2 HCC (GPC3-positive) cells and McA-RH7777 HCC (GPC3-negative) cells were obtained from the Shanghai Institute of Biochemistry and Cell Biology, Chinese Academy of Sciences (Shanghai, China). The cells were cultured in Dulbecco's Modified Eagle's Medium (DMEM) (ThermoFisher Scientific, USA) supplemented with 10% fetal bovine serum (ThermoFisher Scientific, USA). Cells were grown at 37°C in a humidified atmosphere containing 5% CO_2.

All animal experiments were conducted according to the guideline of the Nanfang Hospital Animal Ethics Committee at the Southern Medical University. Male or female

BALB/c nude mice (about 4–6 weeks old) were obtained from the Laboratory Animal Center at Southern Medical University. The HepG2 and McA-RH7777 HCC xenografts were established by subcutaneous injection of 1×10^6 tumor cells into the left shoulder of nude mice. The animals were used for *in vivo* studies when the tumors reached a size of 0.5–1 cm in diameter (4–6 weeks after inoculation).

Binding Assay

The binding affinity of the GP2076 or GP2633 peptide for GPC3 was determined using surface plasmon resonance (SPR) measurements (PlexArray HT A100, Plexera, USA) [1]. In brief, after the GPC3 protein (Novoprotein, China) was immobilized on a 3D Dextran chip, the GP2076 or GP2633 peptide flowed at increasing concentrations (400 nM and 800 nM). The results were analyzed by PlexeraDE software.

In Vitro Biocompatibility

A colorimetric assay was utilized to determine cell viability after treating GPC3 positive HepG2 cells with the GP2076 or GP2633 peptide. The assay was carried out according to the instruction of the manufacturer [2]. In brief, HepG2 cells were seeded at a density of 1×10^4 cells/well in a 96-well plate. After the incubation of the GP2076 or GP2633 peptide at various concentrations (0, 120, 240, 360, 480, 600, 720, and 840 μg/ml) with HepG2 cells for 24 h, the HepG2 cells were examined using the cell counting Kit-8 (KeyGen Biotech, Nanjing, China). The absorbance at 450 nm of all the wells in the 96-well microplate was recorded on a microplate reader (BIOTEK ELX800, USA). The experiment was performed in quadruplicate.

Cellular Uptake, Internalization, and Efflux Studies

Cellular uptake and efflux of Al[^{18}F]F-GP2076 or Al[^{18}F]F-GP2633 in HepG2 or McA-RH7777 cells were performed according to a previously reported protocol [3]. In the cellular uptake study, HepG2 or McA-RH7777 cells were seeded into 12-well plates at a density of 5×10^5 cells per well. After overnight incubation, cells were rinsed 3 times with PBS, followed by the addition of Al[^{18}F]F-GP2076 or Al[^{18}F]F-GP2633 (0.74-1.11 MBq/well) to the wells in

quadruplicate. After incubation at 37°C for 2, 5, 15, 30, 60, and 120 min, cells were rinsed 3 times with PBS and lysed with 0.2 M NaOH containing 1% sodium dodecyl sulfate (SDS). The radioactivity associated with cell lysate was measured by gamma counting. The cell uptake was normalized by the added radioactivity after decay correction.

The internalization assay was carried out similarly to the procedure of cell uptake study except for an additional wash with acid buffer (50 mM glycine, 0.1 M NaCl, pH 2.8) for 1 min, which was conducted after the two PBS washes in order to remove the membrane-bound Al[^{18}F]F-GP2076 or Al[^{18}F]F-GP2633. After the 1 min incubation with the acid buffer, the cells were washed again with cold PBS and removed from the plate. The radioactivity associated with the internalized fraction was measured by gamma counting.

In the cellular efflux study, HepG2 or McA-RH7777 cells were seeded into 12-well plates at a density of 5×10^5 cells per well. After overnight incubation, cells were rinsed 3 times with PBS, and then incubated with Al[^{18}F]F-GP2076 or Al[^{18}F]F-GP2633 (0.74-1.11 MBq/well) at 37°C for 2 h. After the PBS washing and re-incubation with serum-free medium, cells were then washed at different time points (0, 5, 15, 30, and 60 min) with PBS and lysed with 0.2 M NaOH containing 1% SDS. The radioactivity associated with cell lysate was measured by gamma counting. Cell efflux results are presented as percentage of the added dose after decay correction.

In Vitro Stability

The stability of Al[^{18}F]F-GP2076 or Al[^{18}F]F-GP2633 was evaluated in PBS and mouse serum. Briefly, 5.55 MBq of Al[^{18}F]F-GP2076 or Al[^{18}F]F-GP2633 was incubated with 0.5 ml of PBS at room temperature or mouse serum at 37°C with gentle shaking. The stability test was carried out at 2 h after the incubation. For the PBS study, an aliquot of solution was taken, and the radiochemical purity was determined by analytical HPLC. For the mouse serum study, after the addition of TFA, the mixture was passed through a 0.2-μm filter. An aliquot of the soluble fraction was taken, and the radiochemical purity was examined by analytical HPLC.

MicroPET/CT Imaging and Biodistribution

MicroPET/CT scans were carried out using a Siemens Inveon PET/CT scanner (Siemens, Germany). Tumor bearing mice (n = 3/group) were intravenously injected with 5.55 MBq of Al[^{18}F]F-GP2076 or Al[^{18}F]F-GP2633 under isoflurane anesthesia. A ten-minute static PET scan for each animal was acquired at 30, 60, and 120 min after the injection. 3-Dimensional ordered subset expectation maximization (3D-OSEM) algorithm was used for the PET reconstruction, and CT was applied for attenuation correction. Detailed procedures for the microPET/CT imaging and biodistribution are provided in ESM.

Inveon Research Workplace (IRW) 3.0 software (Siemens, Germany) was used to measure the regions of interest (ROIs) determined by superimposing the ellipsoid volume of interest (VOI) on the target tissues. The radioactivity concentrations were measured by the mean pixel intensity within each VOI and converted to dose/ml using a calibration constant. Assuming the tissue density of 1 g/ml, the ROI was then converted to dose per gram and normalized as the percent injected dose per gram (%ID/g). Tumor-to-nontarget uptake ratios, including tumor-to-muscle (T/M), tumor-to-liver (T/L), and tumor-to-kidneys (T/K) ratios, were calculated by dividing the radioactivity uptake in tumor by that in the corresponding normal tissue or organ.

Ex vivo biodistribution was evaluated at 60 min after the tail vein injection of 1.85 MBq of Al[^{18}F]F-GP2076 or Al[^{18}F]F-GP2633. Mice were euthanized and dissected. Major tissues and organs were collected and weighed wet. The radioactivity in the tissues and organs was measured using a gamma counter. The results were presented as %ID/g. For each animal, the radioactivity of the tissue and organ samples was calibrated with a known aliquot of the injected activity. Mean uptake (%ID/g) for a group of animals was calculated with standard deviations.

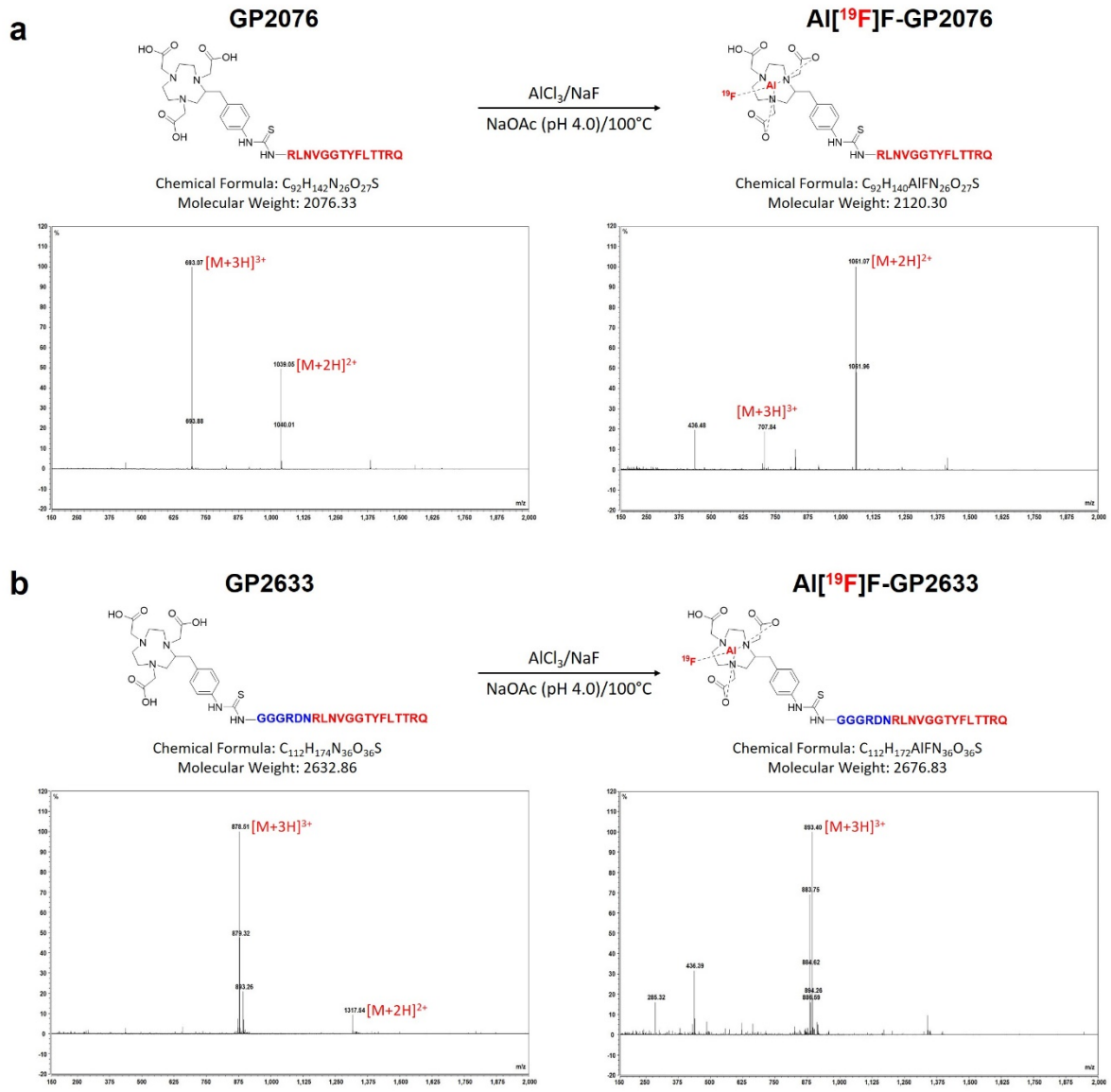

Supplemental Fig. 1. Chemical structures of the peptides are characterized by mass spectrometry. (**a**) The mass spectra demonstrate that Al[^{19}F]F-GP2076 was successfully formed by chelating Al^{19}F to the NOTA of GP2076. (**b**) The mass spectra demonstrate that Al[^{19}F]F-GP2633 was successfully formed by chelating Al^{19}F to the NOTA of GP2633.

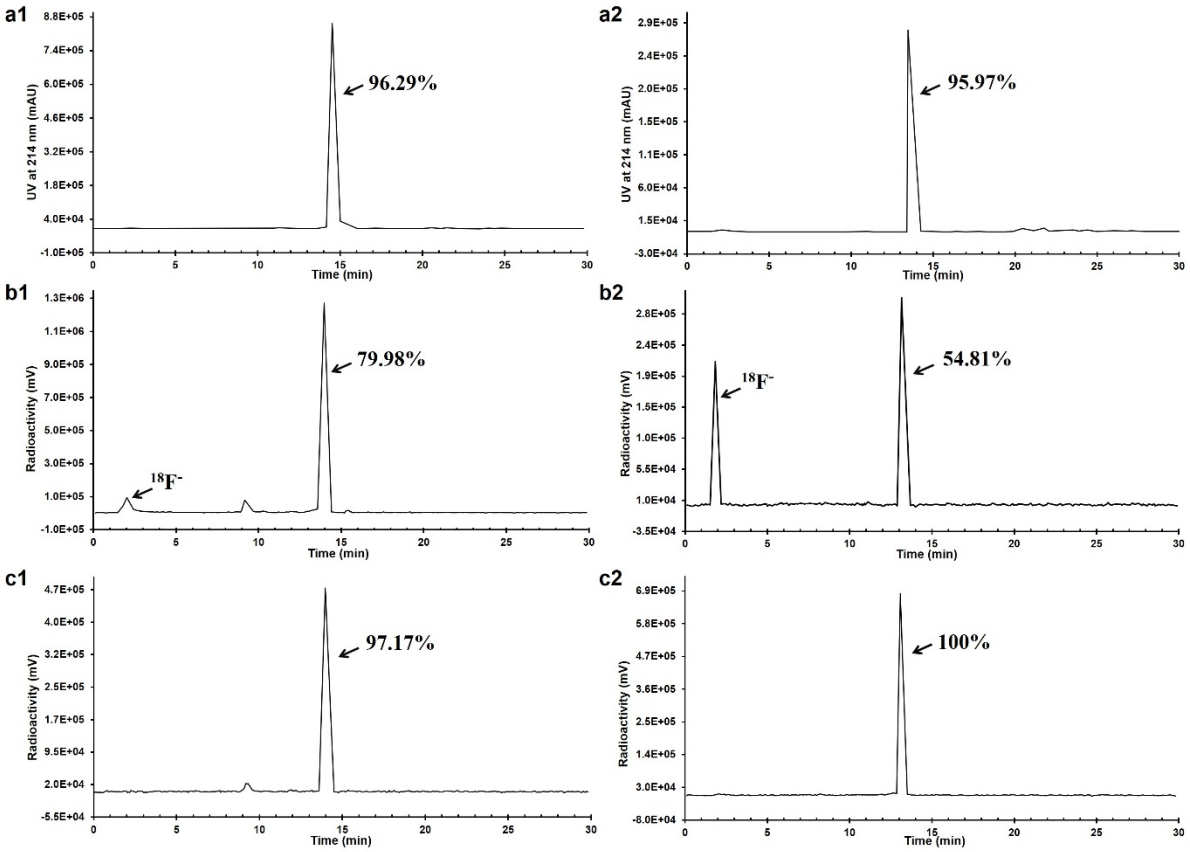

Supplemental Fig. 2. The analytical HPLC UV profile of GP2076 (**a1**) or GP2633 (**a2**) at 214 nm. The analytical HPLC radioactivity profile of the crude product of Al[^{18}F]F-GP2076 (**b1**) or Al[^{18}F]F-GP2633 (**b2**). The HPLC radioactivity profile of Al[^{18}F]F-GP2076 (**c1**) or Al[^{18}F]F-GP2633 (**c2**) after purification.

Supplemental Table 1. Lipophilicity (Log P) of Al[^{18}F]F-GP2076 and Al[^{18}F]F-GP2633.

Peptides	Log P*
Al[^{18}F]F-GP2076	-2.10 ± 0.07
Al[^{18}F]F-GP2633	-2.42 ± 0.09

* The results are presented as mean ± SD (n = 4/peptide).

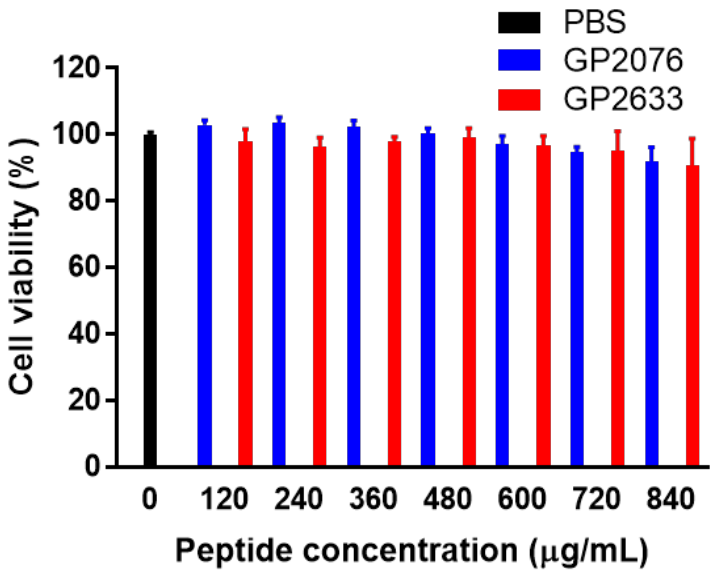

Supplemental Fig. 3. HepG2 cell viability after the incubation with GP2076 or GP2633 at the peptide concentrations of 120, 240, 360, 480, 600, 720, and 840 μg/ml for 24 h. HepG2 cells incubated with PBS were used as a control.

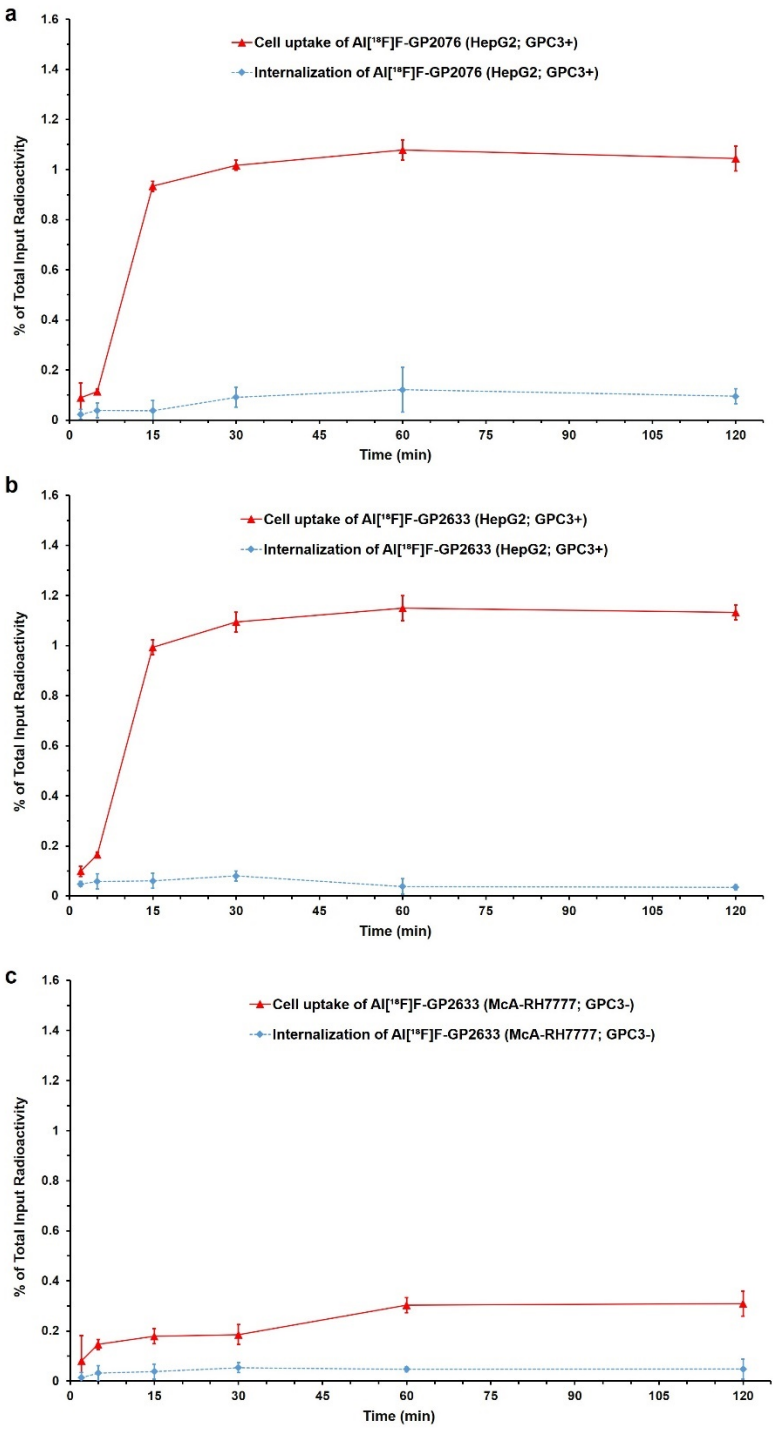

Supplemental Fig. 4. Cell uptake and internalization assay. (**a**) Time dependent cell uptake (red line) and internalization (blue line) of Al[^{18}F]F-GP2076 in GPC3-positive HepG2 cells. (**b**) Time dependent cell uptake (red line) and internalization (blue line) of Al[^{18}F]F-GP2633 in GPC3-positive HepG2 cells. (**c**) Time dependent cell uptake (red line) and internalization (blue line) of Al[^{18}F]F-GP2633 in GPC3-negative McA-RH7777 cells. (n = 4/group, mean ± SD).

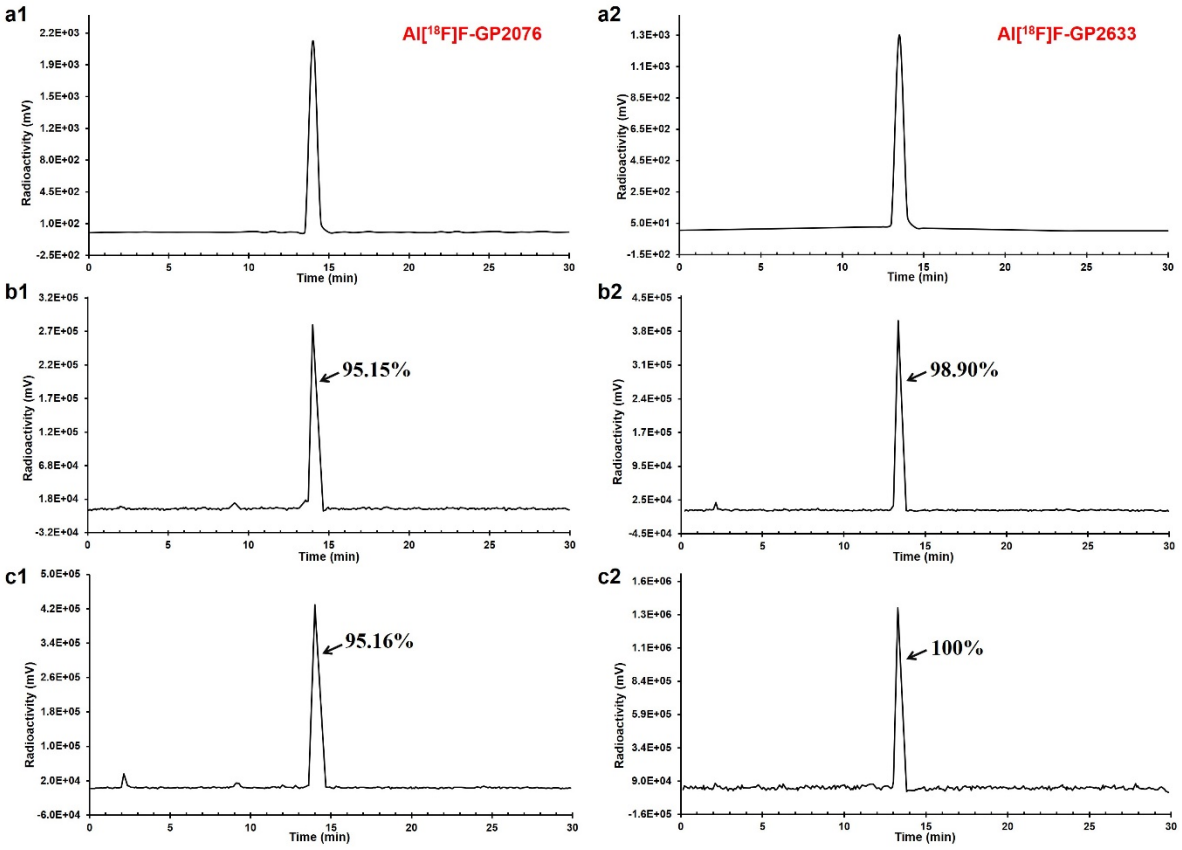

Supplemental Fig. 5. *In vitro* stability of Al[^{18}F]F-GP2076 or Al[^{18}F]F-GP2633 in PBS and mouse serum. The HPLC radioactivity profile of Al[^{18}F]F-GP2076 (**a1**) or Al[^{18}F]F-GP2633 (**a2**) as a reference. The HPLC radioactivity profile of Al[^{18}F]F-GP2076 (**b1**) or Al[^{18}F]F-GP2633 (**b2**) after the incubation of radiolabeled tracers in PBS (pH = 7.4) at room temperature for 2 h. The HPLC radioactivity profile of Al[^{18}F]F-GP2076 (**c1**) or Al[^{18}F]F-GP2633 (**c2**) after the incubation of radiolabeled tracers in mouse serum at 37°C for 2 h.

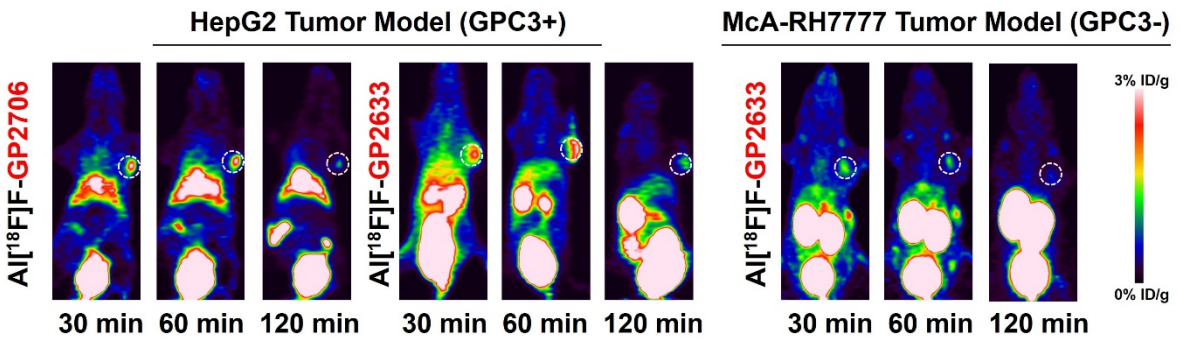

Supplemental Fig. 6. MicroPET images of subcutaneous HCC bearing nude mice after intravenous (i.v.) injection of Al[^{18}F]F-GP2076 or Al[^{18}F]F-GP2633. Tumors are indicated by white circles. Left: Representative decay-corrected whole-body coronal microPET images of nude mice bearing GPC3-positive HepG2 tumor after the i.v. injection of Al[^{18}F]F-GP2076 at 30, 60, and 120 min. Middle: Representative decay-corrected whole-body coronal microPET images of nude mice bearing GPC3-positive HepG2 tumor after the i.v. injection of Al[^{18}F]F-GP2633 at 30, 60, and 120 min. Right: Representative decay-corrected whole-body coronal microPET images of nude mice bearing GPC3-negative McA-RH7777 tumor after the i.v. injection of Al[^{18}F]F-GP2633 at 30, 60, and 120 min.

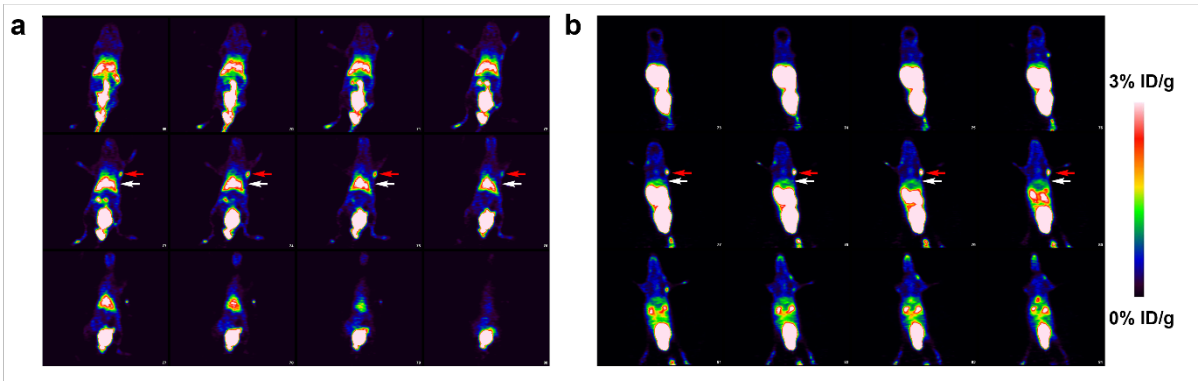

Supplemental Fig. 7. Representative microPET images of continuous whole-body coronal slices of HepG2 tumor bearing mice at 60 min after the i.v. injection of Al[^{18}F]F-GP2076 (**a**) or Al[^{18}F]F-GP2633 (**b**). Tumors are indicated by red arrows, and livers are indicated by white arrows.

Supplemental Table 2. Decay-corrected biodistribution of Al[^{18}F]F-GP2076 or Al[^{18}F]F-GP2633 in HCC bearing nude mice.*

Tissue or Organ	Al[^{18}F]F-GP2076 HepG2 Tumor Model (GPC3+)			Al[^{18}F]F-GP2633 HepG2 Tumor Model (GPC3+)			Al[^{18}F]F-GP2633 McA-RH7777 Tumor Model (GPC3-)		
	30 min	60 min	120 min	30 min	60 min	120 min	30 min	60 min	120 min
	Percent Injected Dose/gram (% ID/g)								
Tumor	2.20 ± 0.36	2.13 ± 0.55	0.73 ± 0.32	3.13 ± 0.31	3.37 ± 0.35	1.30 ± 0.17	1.75 ± 0.05	1.64 ± 0.03	0.66 ± 0.06
Brain	0.63 ± 0.33	0.18 ± 0.13	0.13 ± 0.03	0.10 ± 0.02	0.11 ± 0.02	0.22 ± 0.13	0.78 ± 0.35	0.31 ± 0.16	0.22 ± 0.14
Lung	1.57 ± 0.32	0.78 ± 0.72	0.43 ± 0.18	0.69 ± 0.38	0.59 ± 0.30	0.34 ± 0.04	0.93 ± 0.29	0.74 ± 0.17	0.49 ± 0.12
Heart	1.29 ± 0.45	1.05 ± 0.27	0.36 ± 0.08	1.04 ± 0.32	0.91 ± 0.35	0.37 ± 0.07	1.40 ± 0.40	1.00 ± 0.36	0.47 ± 0.12
Liver	5.10 ± 0.53	3.70 ± 0.98	2.07 ± 0.96	1.80 ± 0.36	1.70 ± 0.26	1.04 ± 0.20	1.52 ± 0.11	1.33 ± 0.06	0.88 ± 0.20
Kidneys	9.83 ± 3.69	7.03 ± 2.32	2.27 ± 1.07	39.40 ± 0.98	36.86 ± 2.05	29.27 ± 3.31	37.47 ± 2.57	35.40 ± 0.92	25.70 ± 3.35
Intestinal	3.03 ± 0.91	2.57 ± 1.16	1.80 ± 1.07	1.09 ± 0.31	1.30 ± 0.10	0.46 ± 0.38	1.43 ± 0.49	1.03 ± 0.25	0.65 ± 0.23
Muscle	0.41 ± 0.09	0.44 ± 0.14	0.28 ± 0.15	0.35 ± 0.04	0.28 ± 0.04	0.22 ± 0.06	0.53 ± 0.25	0.31 ± 0.16	0.20 ± 0.18
Bone	0.95 ± 0.48	0.35 ± 0.21	0.21 ± 0.13	0.47 ± 0.40	0.43 ± 0.49	0.55 ± 0.24	1.04 ± 0.51	0.80 ± 0.26	0.56 ± 0.15

* The results are presented as mean ± SD (n = 3).

Supplemental Table 3. Decay-corrected HepG2 tumor uptake of Al[^{18}F]F-GP2076 or Al[^{18}F]F-GP2633 in HepG2 (GPC3+) tumor bearing mice (n = 3/group).

Time	Al[^{18}F]F-GP2076	Al[^{18}F]F-GP2633	t	*P*
	% ID/g (HepG2 (GPC3+) tumor uptake)			
30 min	2.20 ± 0.36	3.13 ± 0.31	3.421	0.027
60 min	2.13 ± 0.55	3.37 ± 0.35	3.270	0.031
120 min	0.73 ± 0.32	1.30 ± 0.17	2.696	0.054

Supplemental Table 4. Decay-corrected liver uptake of Al[^{18}F]F-GP2076 or Al[^{18}F]F-GP2633 in HepG2 (GPC3+) tumor bearing mice (n = 3/group).

Time	Al[^{18}F]F-GP2076	Al[^{18}F]F-GP2633	t	*P*
	% ID/g (Liver uptake in HepG2 mice)			
30 min	5.10 ± 0.53	1.80 ± 0.36	8.927	0.001
60 min	3.70 ± 0.98	1.70 ± 0.26	3.397	0.027
120 min	2.07 ± 0.96	1.04 ± 0.20	1.817	0.143

Supplemental Table 5. Decay-corrected kidneys uptake of Al[^{18}F]F-GP2076 or Al[^{18}F]F-GP2633 in HepG2 (GPC3+) tumor bearing mice (n = 3/group).

Time	Al[^{18}F]F-GP2076	Al[^{18}F]F-GP2633	t	*P*
	% ID/g (Kidneys uptake in HepG2 mice)			
30 min	9.83 ± 3.69	39.40 ± 0.98	13.406	0.0002
60 min	7.03 ± 2.32	36.86 ± 2.05	16.663	0.0001
120 min	2.27 ± 1.07	29.27 ± 3.31	13.452	0.0002

Supplemental Table 6. Tumor-to-muscle (T/M) uptake ratio of Al[^{18}F]F-GP2076 or Al[^{18}F]F-GP2633 in HepG2 (GPC3+) tumor bearing mice (n = 3/group).

Time	Al[^{18}F]F-GP2076	Al[^{18}F]F-GP2633	t	*P*
	T/M Ratio			
30 min	5.56 ± 1.36	9.11 ± 0.79	3.920	0.017
60 min	5.13 ± 2.08	12.17 ± 0.62	5.621	0.005
120 min	2.68 ± 0.29	6.20 ± 1.80	3.340	0.029

Supplemental Table 7. Tumor-to-liver (T/L) uptake ratio of Al[^{18}F]F-GP2076 or Al[^{18}F]F-GP2633 in HepG2 (GPC3+) tumor bearing mice (n = 3/group).

Time	Al[^{18}F]F-GP2076	Al[^{18}F]F-GP2633	t	*P*
	T/L Ratio			
30 min	0.43 ± 0.06	1.77 ± 0.20	10.824	0.0004
60 min	0.59 ± 0.14	2.00 ± 0.18	10.679	0.0004
120 min	0.46 ± 0.40	1.28 ± 0.25	3.024	0.039

Supplemental Table 8. Tumor-to-kidneys (T/K) uptake ratio of Al[^{18}F]F-GP2076 or Al[^{18}F]F-GP2633 in HepG2 (GPC3+) tumor bearing mice (n = 3/group).

Time	Al[^{18}F]F-GP2076	Al[^{18}F]F-GP2633	t	*P*
	T/K Ratio			
30 min	0.25 ± 0.11	0.08 ± 0.01	2.686	0.055
60 min	0.31 ± 0.04	0.09 ± 0.01	10.273	0.001
120 min	0.46 ± 0.46	0.04 ± 0.01	1.560	0.194

Supplemental Table 9. Decay-corrected tumor uptake of Al[^{18}F]F-GP2633 in HepG2 (GPC3+) vs. McA-RH7777 (GPC3-) tumor bearing mice (n = 3/group).

Time	HepG2 (GPC3+)	McA-RH7777 (GPC3-)	t	*P*
	% ID/g (Tumor uptake)			
30 min	3.13 ± 0.31	1.75 ± 0.05	7.740	0.002
60 min	3.37 ± 0.35	1.64 ± 0.03	8.497	0.001
120 min	1.30 ± 0.17	0.66 ± 0.06	6.038	0.004

Supplemental Table 10. Decay-corrected liver uptake of Al[^{18}F]F-GP2633 in HepG2 (GPC3+) vs. McA-RH7777 (GPC3-) tumor bearing mice (n = 3/group).

Time	HepG2 (GPC3+)	McA-RH7777 (GPC3-)	t	*P*
	% ID/g (Liver uptake)			
30 min	1.80 ± 0.36	1.52 ± 0.11	1.287	0.268
60 min	1.70 ± 0.26	1.33 ± 0.06	2.362	0.077
120 min	1.04 ± 0.20	0.88 ± 0.20	0.982	0.382

Supplemental Table 11. Decay-corrected kidneys uptake of Al[^{18}F]F-GP2633 in HepG2 (GPC3+) vs. McA-RH7777 (GPC3-) tumor bearing mice (n = 3/group).

Time	HepG2 (GPC3+)	McA-RH7777 (GPC3-)	t	*P*
	% ID/g (Kidneys uptake)			
30 min	39.40 ± 0.98	37.47 ± 2.57	1.215	0.291
60 min	36.86 ± 2.05	35.40 ± 0.92	1.130	0.322
120 min	29.27 ± 3.31	25.70 ± 3.35	1.312	0.260

Supplemental Table 12. Tumor-to-muscle (T/M) uptake ratio of Al[^{18}F]F-GP2633 in HepG2 (GPC3+) vs. McA-RH7777 (GPC3-) tumor bearing mice (n = 3/group).

Time	HepG2 (GPC3+)	McA-RH7777 (GPC3-)	t	*P*
	T/M Ratio			
30 min	9.11 ± 0.79	3.87 ± 1.97	4.291	0.013
60 min	12.17 ± 0.62	6.20 ± 2.67	3.782	0.019
120 min	6.20 ± 1.80	5.50 ± 3.65	0.297	0.781

Supplemental Table 13. Tumor-to-liver (T/L) uptake ratio of Al[^{18}F]F-GP2633 in HepG2 (GPC3+) vs. McA-RH7777 (GPC3-) tumor bearing mice (n = 3/group).

Time	HepG2 (GPC3+)	McA-RH7777 (GPC3-)	t	*P*
	T/L Ratio			
30 min	1.77 ± 0.20	1.15 ± 0.09	4.733	0.009
60 min	2.00 ± 0.18	1.23 ± 0.05	6.888	0.002
120 min	1.28 ± 0.25	0.78 ± 0.16	2.935	0.043

Supplemental Table 14. Tumor-to-kidneys (T/K) uptake ratio of Al[^{18}F]F-GP2633 in HepG2 (GPC3+) vs. McA-RH7777 (GPC3-) tumor bearing mice (n = 3/group).

Time	HepG2 (GPC3+)	McA-RH7777 (GPC3-)	t	*P*
	T/K Ratio			
30 min	0.08 ± 0.01	0.05 ± 0.004	6.153	0.004
60 min	0.09 ± 0.01	0.05 ± 0.002	11.040	0.0004
120 min	0.04 ± 0.01	0.03 ± 0.004	3.907	0.017

Supplemental Table 15. Decay-corrected ex vivo biodistribution of Al[^{18}F]F-GP2076 or Al[^{18}F]F-GP2633 in tissues and organs of HepG2 tumor bearing nude mice* at 1 h post-injection.

Tissue or Organ	Al[^{18}F]F-GP2076	Al[^{18}F]F-GP2633
	Percent Injected Dose/gram (% ID/g)	
HepG2 Tumor	1.13 ± 0.02	1.96 ± 0.29
Brain	0.10 ± 0.10	0.12 ± 0.12
Heart	0.36 ± 0.15	0.39 ± 0.27
Liver	2.30 ± 0.56	0.97 ± 0.07
Kidneys	6.37 ± 1.45	37.05 ± 4.70
Muscle	0.24 ± 0.07	0.31 ± 0.05
Blood	0.36 ± 0.17	0.45 ± 0.12
Bone	0.29 ± 0.13	0.36 ± 0.08

* The results are presented as mean ± SD (n = 3).

References

1. Li DL, Tan JE, Tian Y, et al. (2017) Multifunctional superparamagnetic nanoparticles conjugated with fluorescein-labeled designed ankyrin repeat protein as an efficient HER2-targeted probe in breast cancer. Biomaterials 147:86–98
2. Hu K, Wang H, Tang G, et al. (2015) In vivo cancer dual-targeting and dual-modality imaging with functionalized quantum dots. J Nucl Med 56:1278–1284
3. Wu Z, Li ZB, Cai W, et al. (2007) ^{18}F-labeled mini-PEG spacered RGD dimer (^{18}F-FPRGD2): synthesis and microPET imaging of alphavbeta3 integrin expression. Eur J Nucl Med Mol Imaging 34:1823–1831